HHS Public Access

Author manuscript

Radiother Oncol. Author manuscript; available in PMC 2018 September 01.

Published in final edited form as:

Radiother Oncol. 2017 September ; 124(3): 468–474. doi:10.1016/j.radonc.2017.07.018.

Early assessment of dosimetric and biological differences of total marrow irradiation versus total body irradiation in rodents

Susanta Hui[1,2,*], **Yutaka Takahashi**[2,3], **Shernan G. Holtan**[4], **Rezvan Azimi**[2], **Davis Seelig**[5], **Masashi Yagi**[2,3], **Jessie Ingvalson**[5], **Parham Alaei**[2], **Leslie Sharkey**[5], **Behiye Kodal**[2], **Nicholas Peterson**[6], **Carolyn Meyer**[6], **Lindsey Godin**[6], **Michael Ehrhardt**[6], **Guy Storme**[7], **Daohong Zhou**[8], and **Angela Panoskaltsis-Mortari**[6]

[1]Department of Radiation Oncology and Beckman Research Institute, City of Hope, Duarte, CA, USA

[2]Department of Radiation Oncology, University of Minnesota, Minneapolis, MN

[3]Department of Radiation Oncology, Osaka University, Osaka, Japan

[4]Department of Medicine, Division of Hematology, Oncology, Blood and Marrow Transplantation, University of Minnesota, Minneapolis, MN

[5]Department of Veterinary Clinical Sciences – University of Minnesota, St. Paul, MN

[6]Department of Pediatrics, Division of Blood and Marrow Transplantation, University of Minnesota, Minneapolis, MN

[7]Department of Radiotherapy, Universitair Ziekenhuis Brussel, Brussels, Belgium

[8]Department of Pharmaceutical Sciences, College of Pharmacy, University of Arkansas for Medical Sciences, AR, USA

Abstract

Purpose—To develop a murine total marrow irradiation (TMI) model in comparison with the total body irradiation (TBI) model.

Materials and Methods—Myeloablative TMI and TBI were administered in mice using a custom jig, and the dosimetric differences between TBI and TMI were evaluated. The early effects of TBI/TMI on bone marrow (BM) and organs were evaluated using histology, FDG-PET, and cytokine production. TMI and TBI with and without cyclophosphamide (Cy) were evaluated for donor cell engraftment and tissue damage early after allogeneic hematopoietic cell transplantation (HCT). Stromal derived factor-1 (SDF-1) expression was evaluated.

Corresponding author Susanta K Hui, PhD, DABR, Department of Radiation Oncology and Beckman Research Institute, City of Hope, 1500 E Duarte Rd, CA 91010, shui@coh.org.

Conflict of interest

The authors declare no conflict of interest.

Results—TMI resulted in similar dose exposure to bone and 50% reduction in dose to bystander organs. BM histology was similar between the groups. In the non-HCT model, TMI mice had significantly less acute intestinal and lung injury compared to TBI. In the HCT model, recipients of TMI had significantly less acute intestinal injury and spleen GVHD, but increased early donor cell engraftment and BM:organ SDF-1 ratio compared to TBI recipients.

Conclusions—The expected BM damage was similar in both models, but the damage to other normal tissues was reduced by TMI. However, BM engraftment was improved in the TMI group compared to TBI, which may be due to enhanced production of SDF-1 in BM relative to other organs after TMI.

Keywords

total body irradiation; total marrow irradiation; bone marrow transplant; graft-versus-host disease; tissue repair; epidermal growth factor; amphiregulin

Introduction

Total body irradiation (TBI) has been widely used as a standard component of the conditioning regimen for allogeneic hematopoietic cell transplantation (HCT) [1]. In addition to immunosuppression, TBI also provides a measure of leukemic control, especially in acute lymphoblastic leukemia (ALL) [2]. However, traditional TBI exposes un- or minimally involved vital organs, such as the gastrointestinal tract, lungs, eyes, liver, heart and kidneys to significant radiation, contributing to regimen-related toxicity and treatment-related mortality (TRM) [3, 4]. Although a higher TBI radiation dose might overcome the increased risk of relapse, it also increases TRM, resulting in no overall survival benefit [5]. New conditioning strategies that simultaneously facilitate engraftment, provide leukemic control, and minimize organ toxicities are needed.

Given this unmet clinical need, a total marrow irradiation (TMI) protocol was developed and has been evaluated in clinical trials [6–8]. TMI focuses the field of delivered radiation to the bone marrow and other neoplastic foci while sparing non-target adjacent tissues, providing an enhanced therapeutic ratio (dose to sites of disease/dose to vital organs). Thus, it may be possible to increase the radiation dose to the sites of greatest disease burden while sparing less involved tissue to reduce overall pathologic effects. However, because of the lack of preclinical models, there is little understanding of the biological and mechanistic differences between TBI and TMI and their influence on bone marrow engraftment.

To address this gap in knowledge, we first developed a mouse model of TMI to test the hypothesis that TMI would induce less damage to organs but result in a similar marrow response compared to TBI. Then, we developed a clinically relevant TMI and chemotherapy transplant model to test the hypothesis that TMI would result in efficient engraftment while reducing risks of conditioning- and acute graft-versus-host disease-(GVHD)-mediated tissue damage. Furthermore, we analyzed underlying molecular mechanisms of those benefits of TMI by measuring the changes in stromal-derived factor 1 (SDF-1), a chemoattractant associated with successful engraftment [9], as well as epidermal growth factor (EGF) and amphiregulin (AREG), which are growth factors associated with wound healing responses.

Methods

Animal studies were approved by the Institutional Animal Care and Use Committee (IACUC #1106A00461) at the University of Minnesota. All rodents were kept in a standard vivarium and were fed a regular diet and water ad libitum.

Image Guided TMI delivery system

A targeted irradiation jig (TIG) made of Styrofoam was built to deliver TBI and TMI treatments using an X-RAD 320 Biological X-ray Irradiator set up for large-field irradiations [10] (Figure 1A). Radiation exposure time and use of portal film were optimized to distinguish the skeletal system, organs and placement of compensators (Figure 1A ii). TBI was delivered with an open beam, whereas TMI was delivered by adding 2 mm copper compensators on the gut, lungs, and eyes, and placement was verified using XV films. In vivo dose verification was performed using thermoluminescent dosimeters (TLDs) and Gafchromic® EBT3 films. The dose reduction to vital organs was compared with that in our recent clinical TMI study. Further details of the experimental setup are described in Supplemental Methods.

TBI and TMI treatment effect in mice without HCT

BALB/c female mice (14–16 weeks old, Harlan Sprague Dawley, Inc., IN) were divided into 3 groups (6–8 mice per group): no radiation, 8 Gy TBI, and 8 Gy TMI. All mice were anesthetized with an intraperitoneal injection of a ketamine (80 mg/kg)/xylazine (6 mg/kg) anesthetic combination before irradiation. Control mice (no irradiation) were similarly anesthetized. Two days after radiation, the bone marrow and small intestine were evaluated (Figure 1B). Tissues were fixed, embedded in paraffin and evaluated semi-quantitatively for histological changes [11]. Tissue metabolic damage was evaluated in a subset of mice using longitudinal fluorodeoxyglucose (FDG) micro-PET/CT imaging following the method described previously [12, 13].

Allogeneic HCT procedure

Male C57BL/6 mice (14–16 weeks old, Jackson) were used as recipients, and female BALB/c (8–10 weeks old, Jackson) were used as donors for the study (Figure 1B). The recipient mice received either intraperitoneal phosphate buffered saline (PBS) or cyclophosphamide (Cy; Bristol Myers Squibb, Seattle, WA), 120 mg/kg per day as a conditioning regimen pre-HCT on days −2 and −1. At day 0, all mice were irradiated with 8 Gy of TBI or TMI. Recipient mice were transplanted via a caudal vein with 10×10^6 T cell-depleted BALB/c bone marrow. At day 7, mice were euthanized, and the bone marrow was evaluated for donor marrow engraftment of H-$2d^+$ cells by flow cytometry. Marrow and tissue SDF-1 expression in mice receiving TBI versus TMI was evaluated by immunohistochemistry at 3 or 6 days after HCT. GVHD target organs were embedded in OCT, frozen, and analyzed as previously described [14]. Enhanced green fluorescent protein (EGFP) transgenic mice were used as a donor for verification of engraftment using a fluorescence microscope. Details of image-guided TMI development; histological analysis; flow cytometric and optical imaging for engraftment; and measurement of cytokines, chemokines, and growth factors are outlined in Supplemental Methods. Because the

uncertainty of the compensator placement may also reduce the dose to the spleen to 4 Gy (instead of 8 Gy), the effect of two different irradiation doses on the spleen was performed, and no effect on engraftment was demonstrated (Supplement S3).

Statistical Methods

Statistical comparisons across categorical variables were completed using chi-square tests. Differences in continuous variables across categories were completed using Student's t-tests or Kruskal-Wallis tests for non-parametric data [15]. $P < 0.05$ was considered to be significant.

Results

Image Optimization and Radiation Dosimetry

The XV film at low dose (7.5 cGy) exposure provides a reasonable contrast for anatomical guidance identifying compensator placement and the skeletal system (Figure 1A (ii)). Figure 1A (iii) and (iv) show the organ dose distribution measured using TLD and film. With TMI, the dose to vital organs was reduced by 30–50% compared to TBI, whereas the dose to vertebral bone was not affected. The percent of organ dose reductions in TMI for the mouse model were comparable to clinical TMI studies (Supplement S1).

Comparative evaluation of radiation-induced injury after TBI or TMI without HCT

TBI and TMI induced similar myeloablation as indicated by bone marrow (BM) cellularity, cell proliferation (Ki-67 positive cells) and decreases in the number of nucleated BM cells (Figures 2A and B). The TMI mice had less gastrointestinal pathology than TBI mice (Figure 3A). Mice receiving TBI had significantly diminished villus height compared to TMI ($p<0.0001$, unpaired t test). In comparison to the pre-treatment control, the reduction in metabolic activity of the lungs ($p=0.018$), liver ($p=0.024$), and intestine ($p=0.034$) were significant and nearly significant in the femur ($p=0.079$) after TBI (Figure 3B), but non-significant metabolic changes were observed after TMI, indicating a less severe effect of TMI exposure. However, the differences in metabolic activity between TBI and TMI were not significant. EGF expression in the intestine (especially in crypt cells) and expression of IL-10 and SDF-1 in lung tissue was significantly increased after TBI or TMI exposure compared with control mice, but no difference was observed between TBI and TMI (Supplement Figure S2).

Comparative evaluation after HCT

To evaluate the early effect of TMI on donor cell engraftment, we preconditioned mice with TBI or TMI with or without Cy. We found that there was a significant increase in donor BM cell engraftment in the TMI− or TMI+ Cy-treated mice ($p<0.005$) compared to their TBI− or TBI+ Cy-treated counterparts at day 7 after HCT (Figure 4A). To understand the apparent enhanced early engraftment with TMI, we assessed SDF-1 staining of marrow and other organs (Figure 5A). A relative increase in the organ/BM SDF-1 ratio was observed at day 3 in the TBI group compared to TMI (Figure 5B). After day 3, TMI mice had a relatively higher villus height (Figure 6A). The levels of the GVHD-related tissue repair factor EGF and damage factor AREG in the intestine differed significantly from week 1 to week 4, with

EGF decreasing over time and an abnormally elevated AREG/EGF ratio at week 4 in TBI-exposed animals (Figure 6B). EGF levels in TMI treated animals did not differ significantly from controls. Chemotherapy exposure did not impact EGF or AREG protein concentrations in the intestine in either TMI-or TBI-treated mice (not shown). However, EGF significantly decreased over time ($p=0.04$) in comparing TBI week 1 and TBI week 4, resulting in a high AREG/EGF ratio at week 4 in TBI-treated animals. A high AREG/EGF ratio in the intestine in TBI at week 4 is suggestive of unresolved damage and possibly worse GVHD outcomes. In the lung, recipients of TBI had lower EGF compared with levels in TMI, when comparing both groups without chemotherapy exposure. Recipients of TBI + Cy had the lowest AREG compared to TMI + Cy and control animals (Figure 6B). Our observation of Cy exposure with significantly lower AREG levels in TBI-exposed animals, but not TMI-exposed animals, suggesting less physiologic lung tissue repair capacity in recipients of TBI, especially after Cy. There were no differences in classic inflammatory cytokines involved in the pathophysiology of GVHD (TNFα, IL-1b, and IL-17) between these groups (not shown). GVHD histological scores were significantly worse at day 7 in the spleen (median score 2.5 versus median score 1.5, $p=0.03$) in TBI + Cy versus TMI + Cy exposed animals. No TMI recipient had skin GVHD, versus 2 TBI recipients with skin manifestations of GVHD. GVHD histological severity scores did not differ significantly in the gut or liver between TBI or TMI-exposed animals (not shown), despite the observed differences in tissue repair factors in the intestinal tissues.

Discussion

We developed a novel pre-clinical TMI model to complement ongoing clinical TMI investigations used in hematological malignancies globally. We presented dosimetric details of TMI and consequent biological differences with commonly used TBI. In the non-transplant acute phase setting, whereas similar structural and functional changes in the bone marrow were observed after radiation, TMI provided a more protective biological effect, reducing intestinal and lung injury compared to TBI. In the allogeneic transplant setting, mice receiving TMI with or without chemotherapy showed enhanced donor marrow engraftment compared to their TBI counterparts, potentially initiated by the preferential and early activation of the chemo-attractant SDF-1 in the BM.

Marrow myelosuppressive effects were similar in both TBI and TMI treated mice. There were also similarities observed in hematopoietic cell proliferation activity. The difference in BM engraftment efficiency (i.e., lower in TBI and higher in TMI) may be explained by a chemokine gradient phenomenon (schematic presentation in Figure 5B). In TBI, a relative increase in SDF-1 in organs with respect to bone marrow may cause a higher chemokine gradient towards the peripheral niche compared to the BM niche, attracting migratory donor cells from blood to organs and resulting in fewer donor cells being available to reach the BM niche for engraftment. With respect to TMI, the chemokine gradient may be reversed (higher SDF-1 in BM regions relative to non skeletal organs), enabling directional migration of cells towards the BM niche at relatively higher numbers. Our results are consistent with a role for SDF-1α/CXCR4 interactions in hematopoietic stem cell (HSC) homing to bone marrow [9, 16–18].

However, further confirmation will be required to understand the mechanistic role of SDF-1 in TMI settings. It appears that TMI may potentially modulate cell migration by differentially targeting radiation to bone marrow and minimizing induction of SDF-1 expression in other organs. To enhance the efficiency of HCT, TMI could be beneficial and an alternative to direct bone marrow HSC transplantation [19, 20] or glucocorticoid hormone pretreatment [21]. SDF-1 is a chemo-attractant potentially originating from multiple sources, including megakaryocytes, endothelial cells, and osteoblasts [22]. Increased radiation and hypoxia leads to increased SDF-1 [23, 24]. Whether SDF-1 impacts engraftment in the context of increased bone marrow targeted radiation will be of relevance to clinical dose escalation trials [25, 26].

Another aspect of TMI development is to assess early tissue damage and repair. In non-transplanted mice, median villus height was significantly greater in the TMI mice as compared to the TBI mice. Metabolic function of vital organs, as determined by PET scan, may be preserved in TMI mice and could potentially be used as a non-invasive marker, similar to previously reported initiatives to assess organ toxicity by an FDG PET scan [27–30]. Increased recovery of metabolic function after TMI may be a result of the gastrointestinal-protective effect of TMI [31]. These findings indicate significantly less intestinal damage in the TMI mice as compared to the TBI mice. Although the anatomic signature of tissue regeneration will require longer follow up, we attempted to find any early molecular signature, including the role of epidermal growth factor in this context. Both EGF and AREG are essential in the early phase of a wound healing response, but over time an elevated AREG/EGF ratio indicates incomplete tissue repair and is associated with poor outcomes in aGVHD [32, 33]. The TMI model appears to preserve tissue repair capacity, as determined by EGF and AREG, better than TBI exposure. TMI may be an alternative method [e.g., keratinocyte growth factor (KGF) and other approaches] to ameliorate organ injury associated with the conditioning regimen [34]. Future studies will be required to further attenuate lung and intestinal radiation doses to diminish the risk of organ damage, acute and chronic GVHD, and other long-term effects.

The experimental model presented here was limited to a single radiation dose, which does not fully represent how TMI is delivered in clinical trials today with different doses and dose fractions. Moreover, dose enhancement to bone because of photoelectric absorption will occur [35]. However, mice were exposed to the same beam and using the same setup/orientation for both TBI and TMI. A new onboard computed tomography (CT) image-guided TMI system is being developed to enhance speed and dosimetric precision. Further studies to assess the relationship of even greater radiation dose differentials between the marrow and vital organs, and the extent of organ damage over time will be needed to optimize the benefits of TMI. The overarching clinical goal of these studies is to increase therapeutic gain (targeted radiation to bone marrow vs vital organs), to facilitate rapid engraftment and to spare vital organs, while simultaneously reducing relapse risk in patients who are at high risk of both toxicities of transplantation as well as relapse of their hematologic malignancy.

Supplementary Material

Refer to Web version on PubMed Central for supplementary material.

Acknowledgments

This work was supported by the National Institutes of Health (1R01CA154491). The authors acknowledge and thank Professor (Emeritus) Chang Song (University of Minnesota) for helpful advice pertaining to this experiment and Dr. Lucy Brown (City of Hope) on flow cytometry.

References

1. Gilson D, Taylor RE. Total body irradiation. Report on a meeting organized by the BIR Oncology Committee, held at The Royal Institute of British Architects, London, 28 November 1996. Br J Radiol. 1997; 70(840):1201–3. [PubMed: 9505836]
2. Eapen M, et al. Outcomes after HLA-matched sibling transplantation or chemotherapy in children with B-precursor acute lymphoblastic leukemia in a second remission: a collaborative study of the Children's Oncology Group and the Center for International Blood and Marrow Transplant Research. Blood. 2006; 107(12):4961–7. [PubMed: 16493003]
3. Belkacemi Y, et al. Cataractogenesis after total body irradiation. Int J Radiat Oncol Biol Phys. 1996; 35(1):53–60. [PubMed: 8641927]
4. Murdych T, Weisdorf DJ. Serious cardiac complications during bone marrow transplantation at the University of Minnesota, 1977–1997. Bone Marrow Transplant. 2001; 28(3):283–7. [PubMed: 11535997]
5. Clift RA, et al. Long-term follow-Up of a randomized trial of two irradiation regimens for patients receiving allogeneic marrow transplants during first remission of acute myeloid leukemia. Blood. 1998; 92(4):1455–6. [PubMed: 9694737]
6. Hui SK, et al. Helical tomotherapy targeting total bone marrow-first clinical experience at the University of Minnesota. Acta oncologica (Stockholm, Sweden). 2007; 46(2):250.
7. Hui SK, et al. Feasibility study of helical tomotherapy for total body or total marrow irradiation. Med Phys. 2005; 32(10):3214–24.
8. Wong J, et al. Image-guided total-marrow irradiation using helical tomotherapy in patients with multiple myeloma and acute leukemia undergoing hematopoietic cell transplantation. International journal of radiation oncology, biology, physics. 2009; 73(1):273–279.
9. Ratajczak MZ, Suszynska M. Emerging strategies to enhance homing and engraftment of hematopoietic stem cells. Stem Cell Reviews and Reports. 2016; 12(1):121–128. [PubMed: 26400757]
10. Azimi R, et al. Characterization of an orthovoltage biological irradiator used for radiobiological research. Journal of radiation research. 2015 rru129.
11. Hui SK, et al. The influence of therapeutic radiation on the patterns of bone marrow in ovary-intact and ovariectomized mice. PloS one. 2012; 7(8):e42668. [PubMed: 22880075]
12. Yagi M, et al. High-throughput multiple-mouse imaging with micro-PET/CT for whole-skeleton assessment. Phys Med. 2014
13. Yagi M, et al. A Dual-Radioisotope Hybrid Whole-Body Micro-Positron Emission Tomography/Computed Tomography System Reveals Functional Heterogeneity and Early Local and Systemic Changes Following Targeted Radiation to the Murine Caudal Skeleton. Calcif Tissue Int. 2014
14. Blazar BR, et al. Engraftment of severe combined immune deficient mice receiving allogeneic bone marrow via In utero or postnatal transfer. Blood. 1998; 92(10):3949–59. [PubMed: 9808589]
15. Kruskal WH, Wallis WA. Use of Ranks in One-Criterion Variance Analysis. Journal of the American Statistical Association. 1952; 47(260):583–621.
16. Möhle R, et al. The chemokine receptor CXCR-4 is expressed on CD34+ hematopoietic progenitors and leukemic cells and mediates transendothelial migration induced by stromal cell-derived factor-1. Blood. 1998; 91(12):4523–4530. [PubMed: 9616148]

17. Wright DE, et al. Hematopoietic stem cells are uniquely selective in their migratory response to chemokines. The Journal of experimental medicine. 2002; 195(9):1145–1154. [PubMed: 11994419]
18. Wysoczynski M, et al. Incorporation of CXCR4 into membrane lipid rafts primes homing-related responses of hematopoietic stem/progenitor cells to an SDF-1 gradient. Blood. 2005; 105(1):40–48. [PubMed: 15328152]
19. Chen C, et al. Intra-Bone Marrow Transplantation of Endosteal Bone Marrow Cells Facilitates Allogeneic Hematopoietic and Stromal Cells Engraftment Dependent on Early Expression of CXCL-12. Medical science monitor: international medical journal of experimental and clinical research. 2015; 21:2757. [PubMed: 26373579]
20. Futrega K, Lott WB, Doran MR. Direct bone marrow HSC transplantation enhances local engraftment at the expense of systemic engraftment in NSG mice. Scientific reports. 2016; 6
21. Guo B, et al. Glucocorticoid hormone-induced chromatin remodeling enhances human hematopoietic stem cell homing and engraftment. Nature Medicine. 2017; 23(4):424–428.
22. Olson TS, et al. Megakaryocytes promote murine osteoblastic HSC niche expansion and stem cell engraftment after radioablative conditioning. Blood. 2013; 121(26):5238–5249. [PubMed: 23667055]
23. Glass TJ, et al. Stromal cell-derived factor-1 and hematopoietic cell homing in an adult zebrafish model of hematopoietic cell transplantation. Blood. 2011; 118(3):766–774. [PubMed: 21622651]
24. Lerman OZ, et al. Low-dose radiation augments vasculogenesis signaling through HIF-1-dependent and-independent SDF-1 induction. Blood. 2010; 116(18):3669–3676. [PubMed: 20631377]
25. Hui S, et al. Dose Escalation of Total Marrow Irradiation in High-Risk Patients Undergoing Allogeneic Hematopoietic Stem Cell Transplantation. Biology of Blood and Marrow Transplantation. 2017
26. Stein A, et al. Phase I Trial of Total Marrow and Lymphoid Irradiation Transplant Conditioning in Patients with Relapsed/Refractory Acute Leukemia. Biology of Blood and Marrow Transplantation. 2017
27. Hart JP, et al. Radiation pneumonitis: correlation of toxicity with pulmonary metabolic radiation response. International Journal of Radiation Oncology* Biology* Physics. 2008; 71(4):967–971.
28. Mac Manus MP, et al. Association Between Pulmonary Uptake of Fluorodeoxyglucose Detected by Positron Emission Tomography Scanning After Radiation Therapy for Non-Small-Cell Lung Cancer and Radiation Pneumonitis. International Journal of Radiation Oncology* Biology* Physics. 2011; 80(5):1365–1371.
29. O'Farrell AC, et al. A Novel Positron Emission Tomography (PET) Approach to Monitor Cardiac Metabolic Pathway Remodeling in Response to Sunitinib Malate. PloS one. 2017; 12(1):e0169964. [PubMed: 28129334]
30. Yagi M, et al. Longitudinal FDG-PET Revealed Regional Functional Heterogeneity of Bone Marrow, Site-Dependent Response to Treatment and Correlation with Hematological Parameters. Journal of Cancer. 2015; 6(6):531. [PubMed: 26000044]
31. Jia D, et al. Prevention and mitigation of acute death of mice after abdominal irradiation by the antioxidant N-acetyl-cysteine (NAC). Radiation research. 2010; 173(5):579–589. [PubMed: 20426657]
32. Ceafalan LC, et al. Interstitial outburst of angiogenic factors during skeletal muscle regeneration after acute mechanical trauma. The Anatomical Record. 2015; 298(11):1864–1879. [PubMed: 26260512]
33. Holtan SG, et al. Late acute graft-versus-host disease: a prospective analysis of clinical outcomes and circulating angiogenic factors. Blood. 2016; 128(19):2350–2358. [PubMed: 27625357]
34. Ziegler TR, et al. Regulation of glutathione redox status in lung and liver by conditioning regimens and keratinocyte growth factor in murine allogeneic bone marrow transplantation. Transplantation. 2001; 72(8):1354–62. [PubMed: 11685103]
35. Khan, FM., Gibbons, JP. Khan's the physics of radiation therapy. Lippincott Williams & Wilkins; 2014.

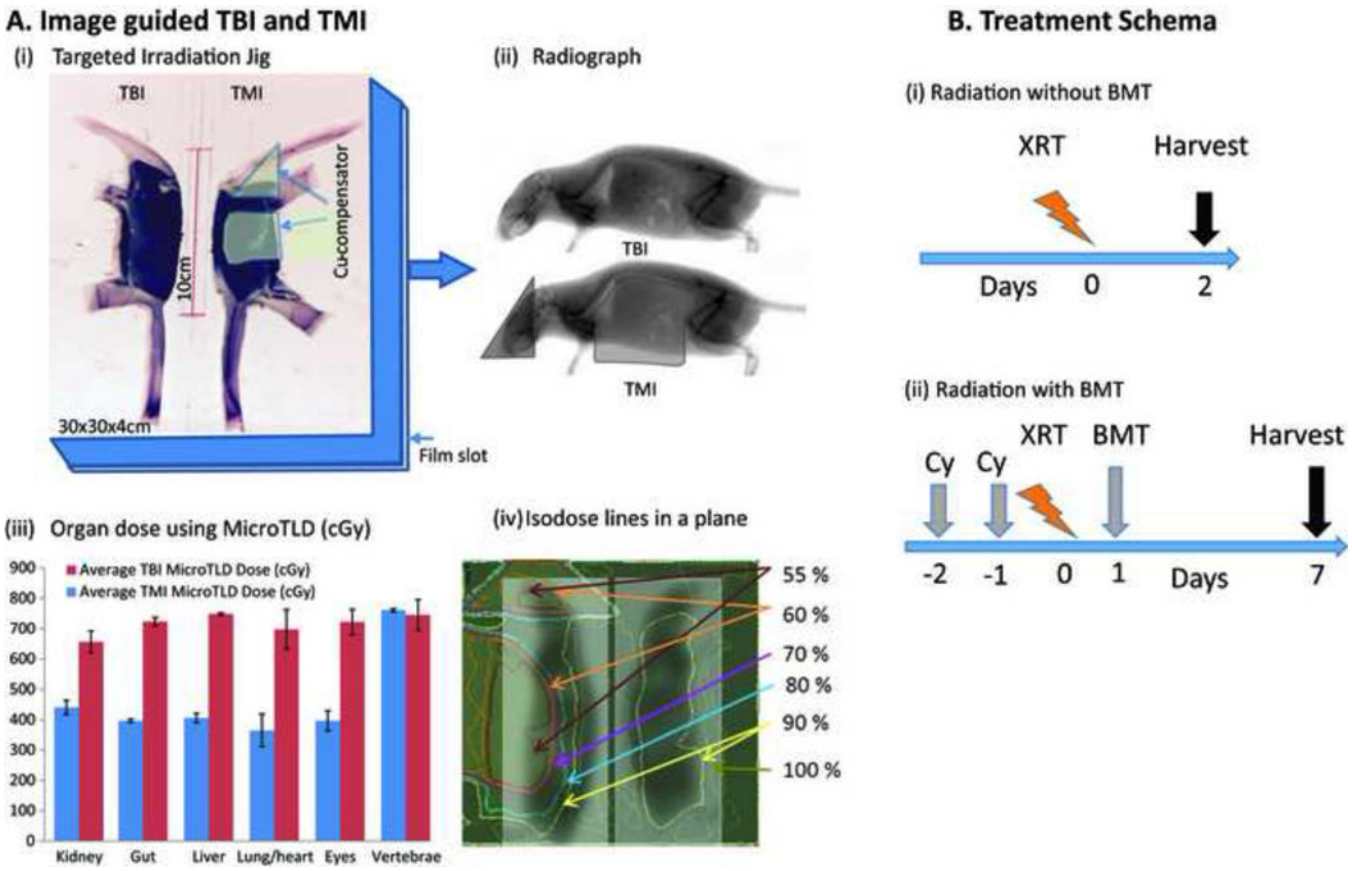

Figure 1.

Schema of image guided total marrow irradiation in mice. A. (i) Targeted Irradiation Jig with accessories, (ii) Radiograph of the mice with and without compensators in the jig, (iii) Organ dose measured using micro TLD, and (iv) isodose lines obtained from the Gafchromic film at the exit. B. Treatment Schema (i) Radiation without bone marrow transplant (BMT) and (ii) Radiation with BMT.

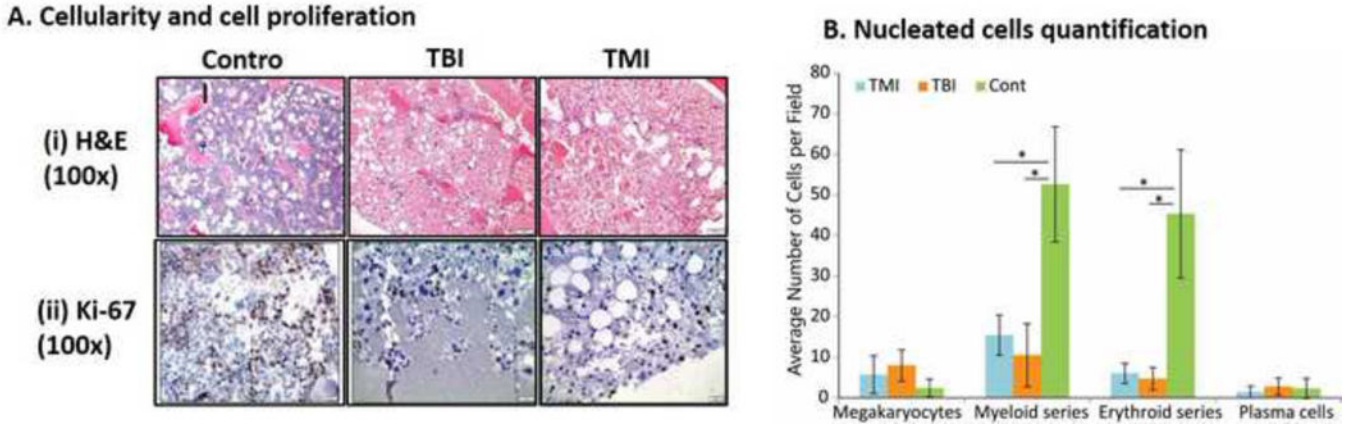

Figure 2.

Demonstration of marrow and serum differences among control, TBI, and TMI treatment conditions using A. Cellularity (H&E), and cell proliferation (Ki67 staining) of bone marrow (femur), B. Nucleated cell quantification presented as average number of cells per field.

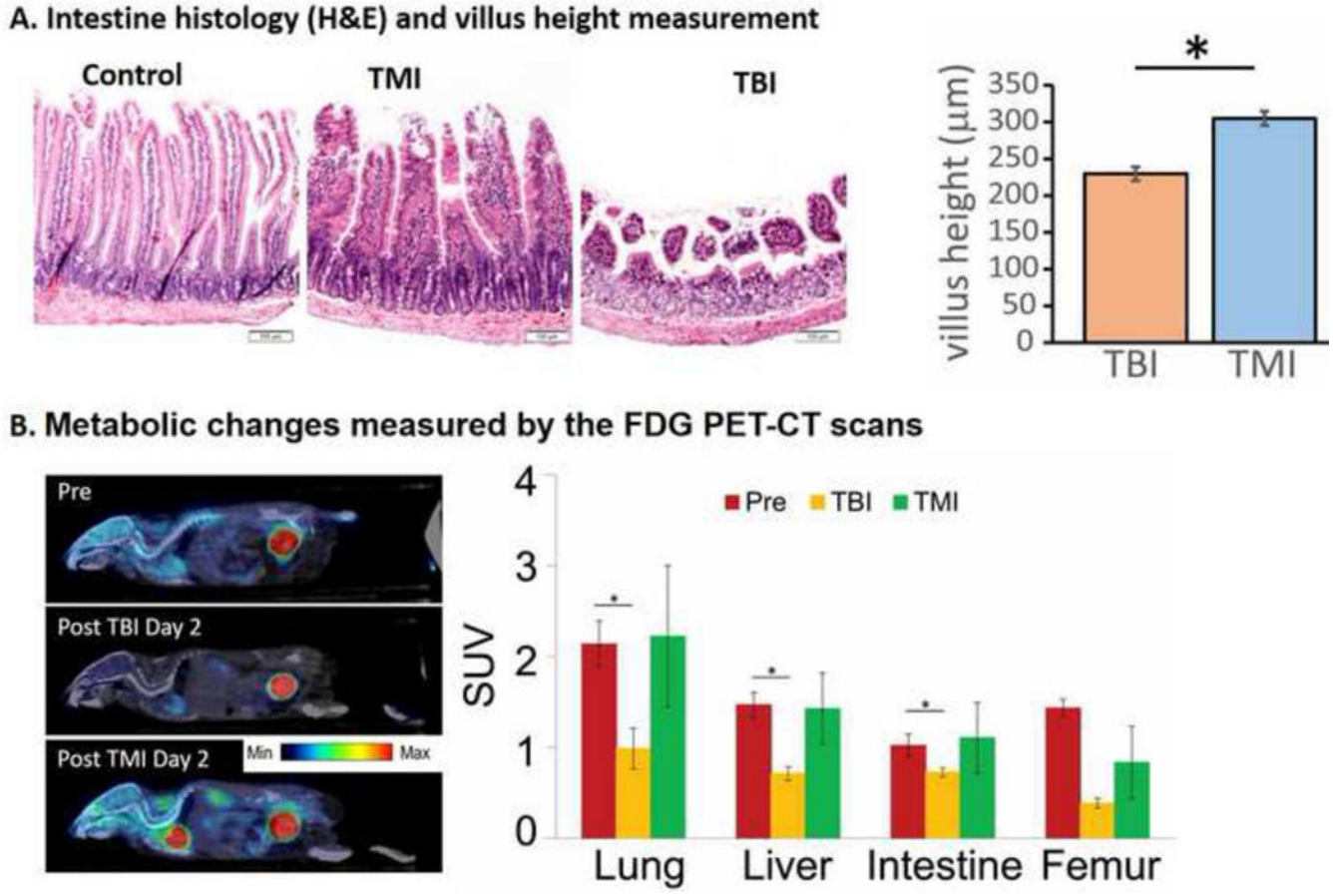

Figure 3.

Demonstration of the differential impact of TBI versus TMI on organs at day 2 without HCT. A intestinal anatomical changes and measurements of villus height and crypt depth, B. Metabolic changes measured by longitudinal PET imaging. Image fusion registration of PET/CT whole body images before and after TBI or TMI and the SUV for various tissues were measured.

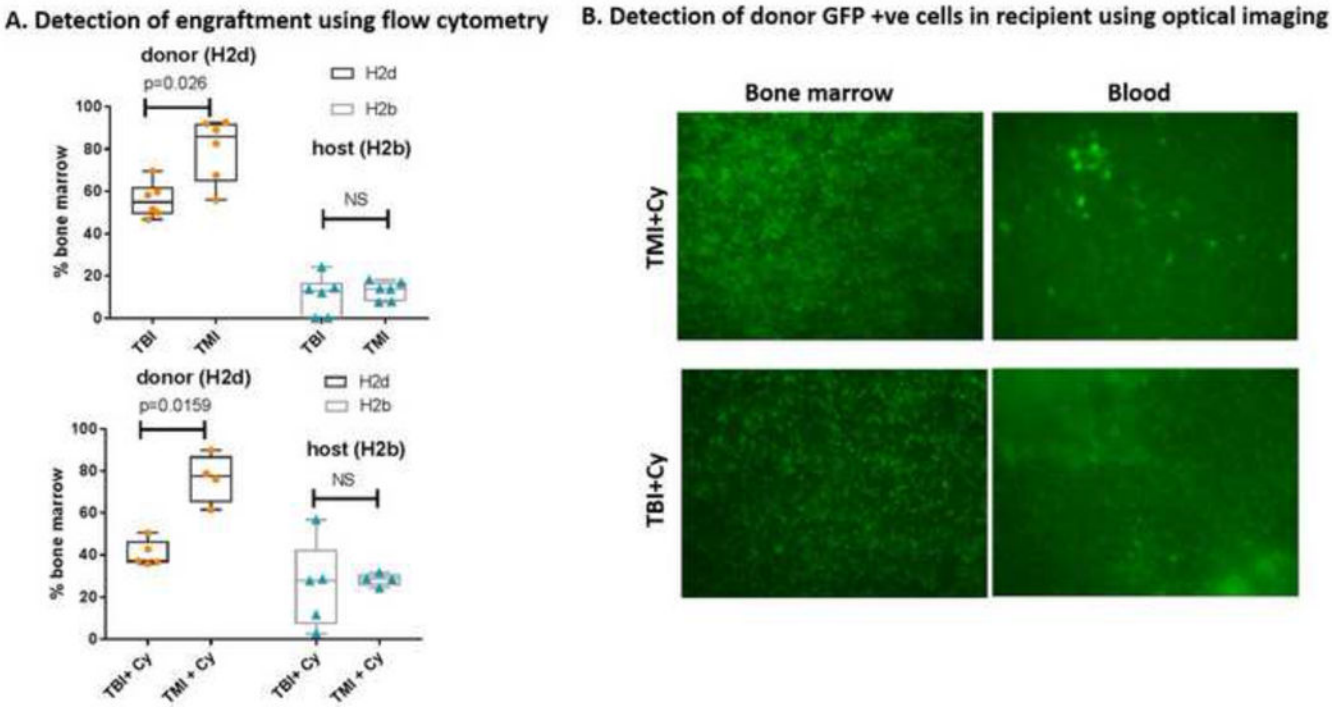

Figure 4.

Bone marrow engraftment (allogeneic transplant model) at day 7 after TMI versus TBI. A. Engraftment pattern for TMI versus TBI with and without chemotherapy (Cy) as monitored by flow cytometry, B. Engraftment as monitored by fluorescence imaging.

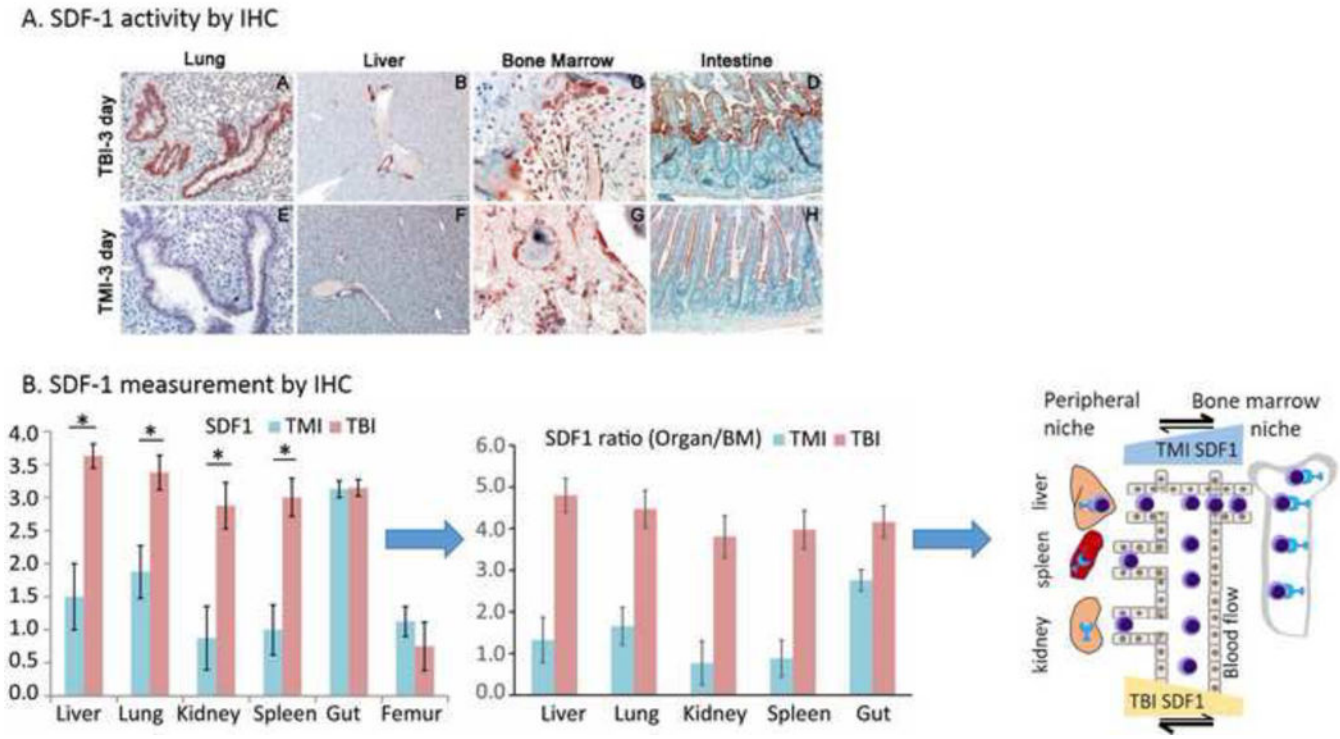

Figure 5.

Intestinal tissue damage assessment and marrow and tissue SDF-1 expression in mice receiving TBI versus TMI, 3 days after HCT. A. Intestinal histology and measured villus height and crypt depth. B. Tissue SDF-1 measurement by IHC is presented for various organs. The derived ratios of SDF-1 in organs with respect to bone marrow are also presented. A schematic presentation showing, for TBI, increased SDF-1 chemokine gradient towards the peripheral niche compared to the BM niche, attracting migratory donor cells from blood to organs; for TMI the reverse migration occurs, with higher chemokine gradient towards the BM niche.

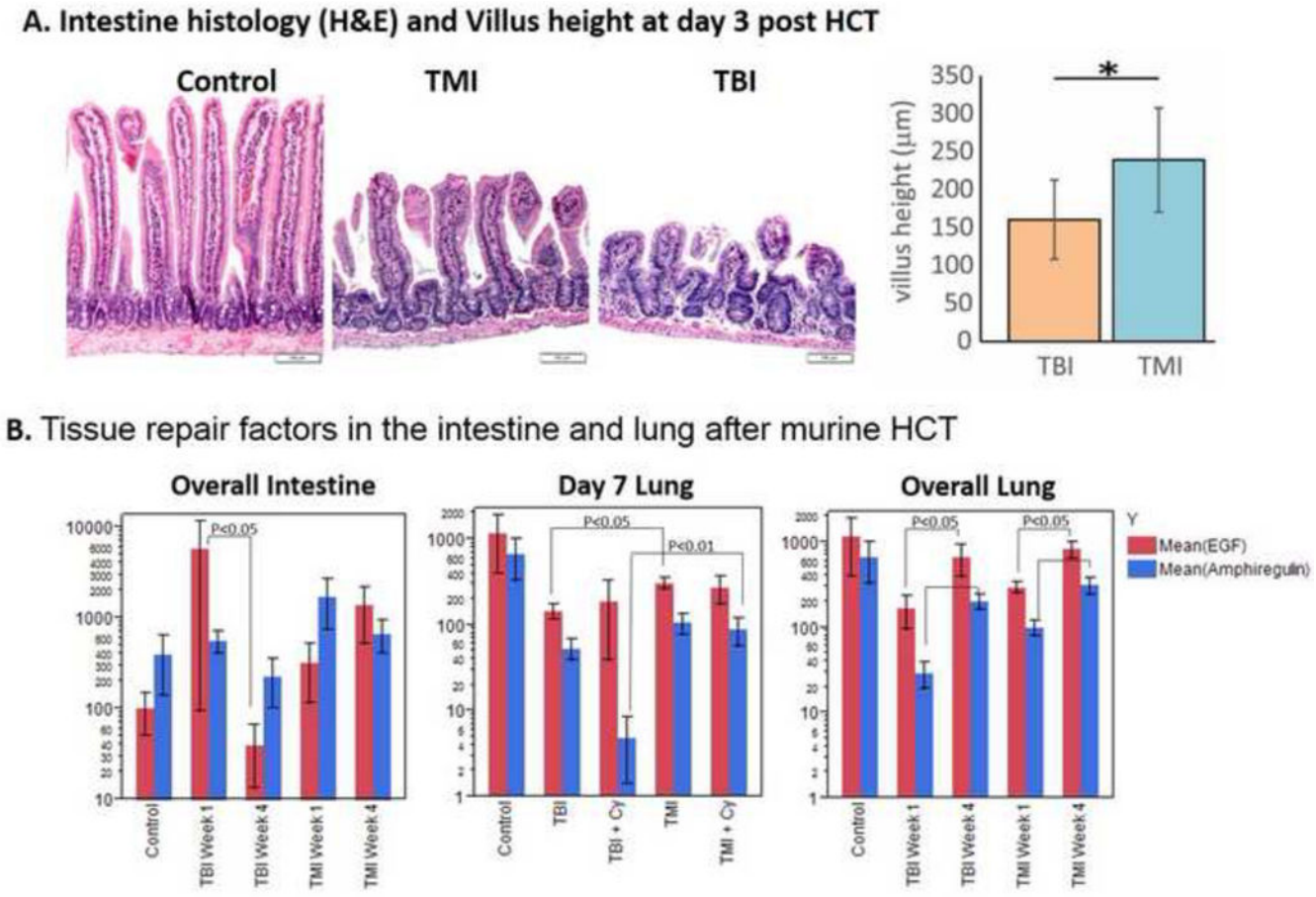

Figure 6.

Tissue damage and repair factors in the intestine and lung after HCT. A. Intestinal histology and measured villus height. B EGF and AREG activity in intestine and lung at week 1 and week 4 after HCT. Bars are mean +/− SEM